Published in final edited form as:

Nat Genet. 2007 February ; 39(2): 189–198. doi:10.1038/ng1928.

PTEN-deficient intestinal stem cells initiate intestinal polyposis

Xi C He[1], **Tong Yin**[1], **Justin C Grindley**[1], **Qiang Tian**[2], **Toshiro Sato**[1], **W Andy Tao**[3], **Raminarao Dirisina**[4], **Kimberly S Porter-Westpfahl**[1], **Mark Hembree**[1], **Teri Johnson**[1], **Leanne M Wiedemann**[1,5], **Terrence A Barrett**[4], **Leroy Hood**[2], **Hong Wu**[6], and **Linheng Li**[1,5]

[1]Stowers Institute for Medical Research, Kansas City, Missouri 64110, USA.

[2]Institute for Systems Biology, Seattle, Washington 98103, USA.

[3]Department of Biochemistry, Purdue University, West Lafayette, Indiana 47907, USA.

[4]Department of Medicine and Microbiology/Immunology, Division of Gastroenterology, Northwestern University Medical School, Chicago, Illinois 60611, USA.

[5]Department of Pathology and Laboratory Medicine, Kansas University Medical Center, Kansas City, Kansas 66160, USA.

[6]Department of Molecular and Medical Pharmacology, University of California, Los Angeles, School of Medicine, Los Angeles, California 90095, USA.

Abstract

Intestinal polyposis, a precancerous neoplasia, results primarily from an abnormal increase in the number of crypts, which contain intestinal stem cells (ISCs). In mice, widespread deletion of the tumor suppressor Phosphatase and tensin homolog (PTEN) generates hamartomatous intestinal polyps with epithelial and stromal involvement. Using this model, we have established the relationship between stem cells and polyp and tumor formation. PTEN helps govern the proliferation rate and number of ISCs and loss of PTEN results in an excess of ISCs. In PTEN-deficient mice, excess ISCs initiate *de novo* crypt formation and crypt fission, recapitulating crypt production in fetal and neonatal intestine. The PTEN-Akt pathway probably governs stem cell activation by helping control nuclear localization of the Wnt pathway effector β-catenin. Akt phosphorylates β-catenin at Ser552, resulting in a nuclear-localized form in ISCs. Our observations show that intestinal polyposis is initiated by PTEN-deficient ISCs that undergo excessive proliferation driven by Akt activation and nuclear localization of β-catenin.

Correspondence should be addressed to L.L. (lil@stowers-institute.org)..

AUTHOR CONTRIBUTIONS

X.C.H., J.C.G. and L.L. designed the research; X.C.H., T.Y., T.S. and J.C.G. performed the research; Q.T., W.A.T. and L.H. performed the mass spectrometry; R.D., K.S.P-W., M.H., T.J. and T.A.B. provided technical support; H.W. contributed critical reagents; J.C.G., L.M.W. and L.L. wrote the paper.

Accession codes. Gene Expression Omnibus (GEO): GSE6078.

URLs. GEO: http://www.ncbi.nlm.nih.gov/projects/geo/.

Supplementary information is available on the Nature Genetics website.

COMPETING INTERESTS STATEMENT

The authors declare that they have no competing financial interests.

The failure of most current therapies to cure cancer has led to the hypothesis that treatments targeted at malignant proliferation spare a more slowly cycling ‘cancer stem cell’ population that has the ability to regenerate the tumor[1]. Recently, cancer stem cells have been identified and shown to seed tumors upon transplantation into a secondary host[2–4]. However, little is known about the process by which mutation(s) in a stem cell result in primary tumor initiation.

Although there are many ‘causes’ of intestinal cancer, it is well established that almost all cases begin with the development of benign polyps, mainly involving benign neoplastic proliferation of epithelium. The epithelium of the small intestine is composed of a proliferation compartment (crypt) and a differentiation compartment in the villus (Fig. 1a). ISCs, located near the crypt base and above Paneth cells[5,6], give rise to enterocytes, goblet cells, enteroendocrine cells and Paneth cells[6–8]. Intestinal polyposis features a substantial increase in the number of crypts (crypt expansion) and a reduction in epithelial cell differentiation[6,7,9,10]. A key question[7,9,11] is whether stem cells are involved in the abnormal crypt expansion during polyp initiation.

Studies of human hereditary intestinal polyposis syndromes (which typically, but not uniformly, predispose affected individuals to gastrointestinal cancers) and equivalent animal models have provided substantial insight into the genetic control of intestinal homeostasis, polyposis and cancer. Polyposis can result from impaired bone morphogenic protein (BMP) signaling[9,10,12] or by overactivation of Wnt–β-catenin signaling[13]. Wnt–β-catenin signaling exerts positive control on multiplication of both stem cells and crypts[13,14], whereas BMP signaling restricts stem cell number and prevents polyposis, in part by suppressing Wnt signaling[9,10].

Cowden disease (OMIM #158350) is a rare autosomal dominant disorder featuring multiple hamartomatous lesions, including intestinal polyps. Cowden disease results from mutation in the gene encoding PTEN[15], a lipid and protein phosphatase that acts as a negative regulator of the phosphatidylinositol-3 kinase (PI3K)-Akt pathway[16]. The roles of PTEN and Akt in intestinal homeostasis and polyposis have not been defined, but there is evidence that they could be key players in the interplay between BMP and Wnt signals. Mutation of *BMPR1A* can result in a Cowden-like syndrome resembling loss of PTEN[17]. BMP signaling may in part be mediated by inhibition of PI3K-Akt activity via positive regulation of PTEN[9,18,19]. In turn, PTEN inhibits, whereas Akt enhances, the nuclear localization of β-catenin[20,21], consistent with our previous model in which Akt assists Wnt signaling in activation of β-catenin in ISCs[9,19].

In this study, we used the PTEN conditional inactivation mouse model[22] to define the role of the PTEN-Akt pathway in the intestine. We implicate PTEN-deficient stem cells in the origin of polyposis and establish a molecular mechanism by which the PTEN-Akt and Wnt–β-catenin pathways coordinate to regulate intestinal homeostasis.

RESULTS

Induced inactivation of PTEN leads to intestinal polyposis

In this study we used the conditional inactivation mouse, model in which exon five of *Pten* is 'floxed' (*Pten*$^{fl/fl}$), to define the role of the PTEN-Akt pathway in the intestine. To determine the time course of PTEN loss, we generated *Mx1-Cre:Pten*$^{fl/fl}$ mice[22] carrying a Z/EG reporter, so that Cre-mediated *Pten* deletion would be reported by the expression of green fluorescent protein (GFP). We induced gene deletion at or before weaning with polyinosinic-polycytidylic acid (pIpC), which provokes innate immune and inflammatory responses and generates interferon that, in turn, activates Cre expression[23]. We first detected GFP$^+$ cells 3 d after completion of pIpC treatment (day 3). Costaining with the stem cell marker Musashi1 (referred to hereafter as 'Musashi')[24] confirmed that recombination had occurred in ISCs (Fig. 1b). Initially, GFP$^+$ epithelial cells were clustered primarily in the crypt bottom or located at the transition zone between crypts and villi (Fig. 1b,c). The GFP$^+$ domains expanded to include groups of crypts on day 5 (Fig. 1d). By day 18, the GFP$^+$ domains encompassed crypts and villi and a minority of the crypts and villi from which PTEN had been lost appeared dysmorphic (Fig. 1e). At day 30, the GFP$^+$ epithelium likewise contained both dysmorphic and apparently normal crypts and villi (data not shown). We found a limited number of stromal cells to be GFP$^+$ (Fig. 1c). We confirmed successful targeting of *Pten* in the intestine by PCR analysis (Fig. 1f), which showed deletion of *Pten* exon 5 encoding the phosphatase motif[22].

We detected multiple polyps (Fig. 1g) in the small intestinal tract of *Pten* homozygous mutant mice (referred to as 'PTEN mutants'; *Mx1-Cre*$^+$*;Pten*$^{fl/fl}$) 1 month after completion of pIpC injection (n = 15) but did not observe them in the control group (*Mx1-Cre*$^+$*;Pten*$^{fl/+}$ or *Mx1-Cre*$^-$*;Pten*$^{fl/fl}$ mice) (data not shown). Histologically, the polyps showed a large excess of crypt-like units at their base as well as an aberrant positioning of crypts along the edges of villi. There were also over-growth and insertions of stromal cells from the base of the polypoid mass, a typical feature of hamartoma[25] (Fig. 1h). The stromal insertions reliably contained smooth muscle α-actin-positive myofibroblasts, whereas the B220-positive lymphocyte component varied from negligible to pronounced (data not shown). Our subsequent analysis of the polyposis focuses on the PTEN mutant epithelium.

PTEN controls cell cycle in intestinal crypts

PTEN inhibits cell proliferation through suppression of PI3K and Akt activity[16]. Therefore, we assessed the proliferation state of cells in the intestinal polyp regions of the PTEN mutants by labeling actively cycling cells with a 3-h pulse of BrdU. In normal crypts, BrdU$^+$ cells were limited to a narrow proliferation zone containing the transit amplifying cells (TACs) (Fig. 1i). However, in PTEN-deficient polyps, the BrdU$^+$ cells were spread widely within the multiple crypt-like structures (Fig. 1j), the proliferating tissue appeared hyperplastic compared with the linear arrangement of proliferating cells in normal crypts (Fig. 1k) and the proliferative index of the epithelial cells (number of BrdU$^+$ cells/(number of BrdU$^+$ cells + number of BrdU$^-$ cells)) was substantially higher (19.4% versus 53.2%; P < 0.01) than in controls (Fig. 1l).

We next examined the relationship between PTEN expression and cell cycle status. PTEN can be phosphorylated at its C terminus by casein kinase II, which impairs its recruitment to the plasma membrane, where it antagonizes PI3K-Akt activity[26]. Thus, the most active forms of PTEN are nonphosphorylated but can be detected by a phosphorylation-insensitive antibody (pan-PTEN). We found pan-PTEN immunostaining in two distinct cell populations. Multiple pan-PTEN–positive cells were present in a portion of crypt TACs, the majority of which were $BrdU^-$ (Fig. 2a,b). We also observed pan-$PTEN^+$ $BrdU^-$ cells toward the base of the crypt in the expected ISC location (Fig. 2a,c). The presence of PTEN expression in the less actively proliferating cells of the crypt, along with the increase in the proportion of proliferating cells in PTEN mutants, suggests that PTEN acts in TACs as a negative regulator of the cell cycle.

In our mutants[22], loss of PTEN function is expected to result in activation of Akt (as measured by the phosphorylated form of Akt-Thr473 (hereafter 'p-Akt') and phosphorylation of the Akt downstream target GSK3β at Ser9 ('p-GSK3β')[16]. Indeed, protein blot analysis demonstrated increased levels of p-Akt and p-GSK3β in the PTEN-deficient mice (Fig. 2d). We found that cyclinD1 and c-Myc, two downstream targets of the PI3K-Akt pathway[27] that are important for G_1/S phase transition, were upregulated (Fig. 2d) in intestines from PTEN-deficient mice relative to controls. By microarray analysis, we identified genes with the ontology term 'regulation of cell cycle' that were upregulated or downregulated (more than twofold) in PTEN-deficient polyp areas compared with control intestine (Fig. 2e). This uncovered coordinated changes in gene expression in the PTEN mutants: notably, upregulation of *Ccnd3* (which encodes cyclinD3) and *Cdk6* (encoding a cyclinD interacting factor) and increased expression of several key genes involved in the cell cycle G_1/S checkpoint (Fig. 2e). Downregulation of *JunB* in PTEN mutants is notable, as phenotypic similarity between PTEN and JunB mutants in hematopoetic stem cells suggests a functional link between these genes[28,29].

In summary, the increased proliferation rate in the polyps of PTEN mutants is attributable to a requirement for PTEN as a negative cell cycle regulator within the TACs of the crypt. Loss of PTEN results in increased Akt activity and increased expression of cyclinD1, *Myc* and additional genes acting at the G_1/S transition.

Musashi$^+$ stem and progenitor cells initiate polyp formation

The observations that PTEN is expressed in ISCs (Fig. 2c; ref. 9) and that PTEN loss results in polyposis raise the possibility that PTEN-deficient ISCs are responsible for polyp formation. To test this hypothesis, we tracked ISCs using the marker Musashi[24]. In normal intestinal crypts, we detected two classes of $Musashi^+$ cells by a polyclonal antibody to Musashi (anti-Musashi) (Chemicon; cat. no. AB5977). As expected, we detected many $Musashi^+$ crypt cells at the ISC position and found that they could be costained for long-term retention of BrdU (BrdU-LTR) (Fig. 3a), but we also observed some isolated $Musashi^+$ BrdU-LTR^- cells (potentially progenitor cells) higher in the crypt (Fig. 3a) and in the transition zone between crypt and villus (Supplementary Fig. 1 online). Rat monoclonal anti-Musashi yielded a slightly broader pattern of signal but had a similar distribution of strongly positive cells[24] (Supplementary Fig. 2 online). The enhanced BrdU-LTR in

Musashi$^+$ ISCs, compared with progenitors, suggests that the ISCs are more frequently in a prolonged quiescent state. Nevertheless, Musashi$^+$ 'progenitors' shared multiple molecular characteristics with ISCs (see below and Supplementary Fig. 1) and will be considered together as 'Musashi$^+$ ISCs and progenitors' (M$^+$ISC/p). To support ongoing intestinal regeneration, ISCs need to be able to change from quiescence to an active state in which they can undergo division. PTEN-deficient M$^+$ISC/p cells cycle far more often than their normal counterparts: the proliferation cell marker Ki67 labeled 24% of the M$^+$ISC/p cells with mutant *PTEN* but labeled only 2%–4% of the control M$^+$ISC/p cells (Fig. 3b–d). This marked increase in proliferation may reflect an increased rate of cell cycle entry, more rapid progression or both.

Crypt expansion in colon cancer and polyposis can be caused by 'bottom-up' crypt fission (division of an existing crypt starting at its base), or by 'top-down' *de novo* crypt formation (budding of a new crypt from a crypt or villus)[9,10,30–33]. We found that both mechanisms of crypt expansion occurred in PTEN-deficient intestines and were associated with an excessive production of M$^+$ ISC/p cells (Fig. 3e–o).

Dissociation of PTEN-deficient polyps showed that crypts were undergoing fission (Fig. 3e) or budding (Fig. 3i) at a significantly higher rate than in controls (Fig. 3l). M$^+$ISC/p cells, a rare population of cells in normal intestine (Supplementary Fig. 1), still formed only a minor component of the PTEN-deficient polyps but were found in clusters that seemed to be seeding the formation of new crypts. In examples of crypt fission, we observed M$^+$ISC/p cells forming the apex of the ridge between crypts, suggesting that these cells are central to the fission process (Fig. 3f–h and **Supplementary Fig. 3** online). In the *de novo* formation of crypt-like structures in either crypts or villi (crypt budding), we found that small branches in the polyps (newly forming crypts) (Fig. 3j,k,m,n and **Supplementary Fig. 3**) contained pairs or small groups of M$^+$ISC/p cells along with other cycling and noncycling cells, suggesting stem cell–directed growth (Fig. 3k,n,o). We also observed groups of Musashi$^+$ cells in villi where invagination was being initiated (Fig. 3j and **Supplementary Fig. 3**). Hence, in both crypt fission and crypt budding, we found Musashi$^+$ cells at the initiation points of newly forming crypts (Fig. 3h,o).

PTEN-Akt pathway linked to ISC/p cell number and behavior

To help define the molecular link between loss of PTEN and a change in ISC/p cell behavior, we focused on the pathways downstream of PTEN-Akt leading to β-catenin–dependent transcription and cell cycle entry and progression (Fig. 4). The phosphorylated forms of PTEN and Akt, along with the adaptor protein 14-3-3ζ, have been found in ISCs[9,19]. Extending these findings, we found that cells in the ISC position, as well as a limited number of progenitor cells higher in the crypt, were highly positive for phosphorylated PTEN (p-PTEN), p-Akt, p-GSK3β, 14-3-3-ζ and Musashi (Fig. 4a–e,h and Supplementary Fig. 1). We observed lower amounts of p-Akt and p-GSK3β signal in the adjacent TACs (Fig. 4e,h). Thus, a portion of M$^+$ISC/p cells have high Akt[9] activity and correspondingly high amounts of p-GSK3β. Similar colocalization studies established that ISCs with high Akt activity (p-Akt$^+$ or p-PTEN$^+$) were commonly strongly positive for

nuclear cyclinD1 and nuclear Cdkn1b or nuclear plus cytoplasmic Cdkn1b ($p27^{Kip1}$) (Fig. 4c,d).

In PTEN-deficient polyps, cells intensely positive for p-Akt and p-GSK3β were more frequent and were found at different depths within the same crypt and in unusual clusters (Fig. 4f,g,i,j). Staining of adjacent sections showed a close correspondence between the two markers (Fig. 4g,j). Thus, loss of PTEN function increases the number and alters the distribution of ISC/p cells engaged in active Akt signaling.

Phosphorylation by Akt inactivates GSK3β, helping the Wnt signal to permit β-catenin to escape proteasome-mediated degradation and facilitating its nuclear translocation and involvement in transcriptional regulation[21] (Fig. 4u). We assessed β-catenin–mediated transcriptional activity using the transgenic reporter Top-Gal, in which β-catenin and T cell factors (TCFs) cooperatively drive β-galactosidase expression. In PTEN mutants, the number of Top-Gal^{+} cells was increased, and we detected Top-Gal expression, normally a property of ISCs or Paneth cells, ectopically in the villi (Fig. 4k–m and **Supplementary Fig. 4** online).

Akt might promote M^{+}ISC/p cell proliferation by upregulating the expression of cyclinD1 by means of the mammalian target of rapamycin (mTor) or via enhanced β-catenin activity[27,34]. Another possible mechanism is inactivation of the cycle-dependent kinase inhibitor $p27^{kip1}$, as phosphorylation of $p27^{kip1}$ by Akt at Thr157 induces its nuclear export[35] (Fig. 4v).

A high amount of nuclear-localized cyclinD1 is normally a property of the relatively slow-cycling ($Ki67^{-}$) M^{+}ISC/p cells, whereas lower amounts of cyclinD1 are found in the more proliferative TACs (Fig. 4n and **Supplementary Fig. 4**). Mirroring the changes in active Akt signaling and Top-Gal activity, PTEN-deficient polyps contained an abnormally high number and disorganized cluster arrangement of cells with high levels of nuclear cyclinD1 (Fig. 4o,p). Likewise, there was a higher number and altered distribution of cells with nuclear $p27^{kip1}$ (Fig. 4q–s). Owing to the limited performance of available antibodies, we were unable to determine the Thr157 phosphorylation status of $p27^{kip1}$ in tissue sections, but by protein blot we found that PTEN deficiency in the intestine resulted in an overall increase in both $p27^{kip1}$ and Thr157-phosphorylated $p27^{kip1}$ (Fig. 4t). Together, these results are consistent with the loss of PTEN (i) increasing the numbers of stem and progenitor cells, (ii) increasing the proportion of such cells with high amounts of nuclear cyclinD1 and/or nuclear $p27^{kip1}$ or (iii) affecting both the number and cell cycle status of this cell population.

Akt phosphorylates the C terminus of β-catenin at Ser552

In a variety of systems, including the intestine, nuclear localization of β-catenin is believed to be a key event in stem cell activation[9,36]. Thus, we sought to define the interaction between the PTEN-Akt pathway and β-catenin nuclear localization. We have proposed that Akt coordinates with Wnt signaling and assists in the activation of β-catenin in ISCs[9], either through phosphorylation of GSK3β (ref. 37) or by phosphorylation of β-catenin itself[19].

We identified a putative Akt phosphorylation site at Ser552 (Fig. 5a), and lower-stringency searches identified additional putative Akt sites at Thr217, Thr332 and Ser675 (data not shown). Using a liquid chromatography–mass spectrometry assay, we found that Ser552 of β-catenin is phosphorylated by Akt *in vitro* (Fig. 5b,c). The phosphorylation of β-catenin by Akt can prime β-catenin for 14-3-3ζ binding and further stabilization[19]. The Arg-Arg-Thr-Ser sequence containing Ser552 forms a phosphoserine motif that serves as an optimal recognition site for 14-3-3ζ (ref. 38).

To assay for β-catenin phosphorylated by Akt at Ser552, we developed and characterized a phospho-specific antibody (anti-p-β-cat-Ser552). In immunoprecipitation experiments (Fig. 5d) performed with purified intestinal crypts, anti-p-β-cat-Ser552 precipitated forms of β-catenin that could be recognized by an existing antibody that recognizes β-catenin not phosphorylated at the N terminus, which is typically enriched in the nucleus[39]. This indicates that intestinal crypts contain a population of β-catenin molecules that are phosphorylated on Ser552 but not phosphorylated at the N terminus. On protein blots, anti-p-β-cat-Ser552 detected β-catenin, as expected, and we obtained efficient blocking of the signal when we preincubated the antibody with a phosphopeptide for the antigen but not when we used the equivalent non-phosphopeptide, indicating that the antibody is phospho-specific (Fig. 5e). Use of this antibody demonstrated that polyps of PTEN mutants had higher levels of β-catenin phosphorylated at Ser552 (p-β-cat-Ser552) than control intestine (Fig. 5e).

Nuclear localization of β-catenin phosphorylated at Ser552

We next explored the relationship between Ser552 phosphorylation and β-catenin nuclear localization and activity (Fig. 6). Nuclear extracts of intestinal crypts contained p-β-cat-Ser552, and we detected higher levels in PTEN mutants than in controls (Fig. 6a). Immunohistochemistry showed strong spatial and subcellular localization of anti-p-β-cat-Ser552, with intense nuclear signal present in ISC/p cells and occasionally also in Paneth cells (Fig. 6b and **Supplementary Fig. 4**). The antigen peptide blocked this signal, confirming the specificity of the antibody (Fig. 6c). We also observed cells with lower levels of signal in a perinuclear pattern in some crypt cells (**Supplementary Fig. 4**). Consistent with our immunoprecipitation experiments, the active (that is, not phosphorylated at the N terminus) and p-β-cat-Ser552 forms of β-catenin exhibited similar distributions in intestinal crypts. We observed N-terminally nonphosphorylated β-catenin in the nuclei of M^+ISCs (Fig. 6d), in dividing ISCs (Fig. 6f) and in a subset of cells in other crypt positions (for example, in the Paneth cell in Fig. 6f). The antibody to the p-β-cat-Ser552 form likewise detected nuclear β-catenin in $Ki67^-$ ISCs (Fig. 6e) and in dividing ISCs (Fig. 6g) but also in cells at other crypt positions (**Supplementary Fig. 4**). Regardless of the antibody used, we observed ISCs with nuclear β-catenin undergoing division perpendicular to the plane of the epithelium (a feature of asymmetric division) and in close proximity to a mesenchymal cell (a putative stem cell niche) (Fig. 6f,g). In pairs of asymmetrically dividing or recently divided ISCs (based on the expression of Musashi or nuclear $p27^{kip1}$ and on relative position), both cells were usually positive for nuclear p-β-cat-Ser552, but we also occasionally observed pairs of nuclear $p27^{kip1}$-positive cells in which only the cell distal to the mesenchymal cell had nuclear p-β-cat-Ser552 (**Supplementary Fig. 4**). Use of

alternative β-catenin antibodies in costaining experiments showed that ISCs could also have a membranous or cytoplasmic, rather than nuclear, distribution of β-catenin (**Supplementary Fig. 4**).

For cells in the ISC position, but not for Paneth cells, we found that Top-Gal expression was strongly correlated with Akt activity (Fig. 6h,i) and p-β-cat-Ser552 nuclear localization (Fig. 6j,k). This was most readily apparent in PTEN mutants, in which ISCs are more frequently positive for p-Akt, p-β-cat-Ser552 and Top-Gal activity. Based on our biochemical and immunostaining data, we propose a molecular pathway by which the Wnt and PTEN-Akt pathways interact to control β-catenin nuclear localization and transcriptional activity in the M^+ISC/p cell (Fig. 6l). In these cells, β-catenin exists in a range of states, and the nuclear forms may lack phosphorylation at the N terminus, may be phosphorylated towards the C terminus by Akt or may have both of these properties (Fig. 6m).

Cells with nuclear p-β-cat-Ser552 initiate crypt expansion

In PTEN-deficient polyps, we observed that cells with nuclear p-β-cat-Ser552 were greater in number and abnormally localized (Fig. 7 and **Supplementary Fig. 5** online), similar to our findings with Musashi and with markers of an active Akt pathway. Per unit length of intestine, the PTEN-deficient polyps contained twice as many cells with a nuclear anti-p-β-cat-Ser552 signal as in control intestines (**Supplementary Fig. 5**). PTEN loss had less effect on the number of such cells per crypt, suggesting that the overall increase is correlated with the increased number of crypts per unit length in the mutants. Consistent with this relationship, in the PTEN mutants, the cells with nuclear p-β-cat-Ser552 were frequently clustered together and were found at sites of crypt fission (Fig. 7a,b) and at sites of invagination where new crypts were budding from the sides of villi or crypts (Fig. 7c). Because fission and budding can be difficult to recognize from sections, we isolated examples of crypt fission or budding from the mutant polyps and then used immunofluorescence and confocal microscopy to identify cells with nuclear p-β-cat-Ser552. In crypt fission samples, we found cells with nuclear p-β-cat-Ser552 at the apex of the ridge dividing the crypts (Fig. 7d **and Supplementary Video 1** online). In crypt budding, they were present at the junction between newly forming and parent crypts (Fig. 7e and **Supplementary Video 2** online).

DISCUSSION

PTEN-Akt pathway controls ISC/p cell proliferation

The mouse model presented here recapitulates Cowden disease in humans, in which PTEN mutations are associated with the development of multiple hamartomatous lesions featuring contributions from both epithelial and stromal cells[15,25]. Focusing on the crypt, we have determined that PTEN acts as a negative regulator of cell cycle in ISC/p cells and TACs, a role consistent with the pattern of PTEN expression within crypt epithelium. Polyps ultimately occupy only a small fraction of the mutant epithelium. Thus, polyp formation is not solely a consequence of epithelial PTEN loss, but rather involves some additional components or events. Mx1-Cre is able to induce gene deletion in multiple tissues and is activated by provoking an immune response. Thus, our model provides a novel platform in

which to explore key issues in gastrointestinal disease, such as interaction between inflammation and the initiation or progression of neoplasia. Future studies, perhaps involving tissue-specific Cre lines, should help elucidate the role of stromal cells and dissect additional contributions to the intestinal lesions.

M^+ISC/p cells are a slow-cycling cell population, usually either quiescent (G0) or in prolonged G1, when they show a typical signature of nuclearly localized cyclinD1, $p27^{kip1}$ and β-catenin. Loss of PTEN markedly increases the proportion of M^+ISC/p cells that are more actively cycling and also increases the number of M^+ISC/p cells with enhanced Akt signaling coupled to nuclearly localized β-catenin, cyclinD1 and $p27^{kip1}$. We propose that the PTEN-Akt pathway governs M^+ISC/p cell activation, proliferation and number by cooperating with the Wnt pathway to control nuclear localization of β-catenin and, hence, the regulation of β-catenin targets such as cyclinD1. Akt phosphorylation of $p27^{kip1}$ may also be involved in promoting the transition from G1 to S. Under normal conditions, expression of non-p-PTEN in a subpopulation of TACs actively inhibits PI3K and Akt and restrains their cellular proliferation. The increased proportion of cells in S phase in PTEN-deficient polyps and our molecular findings are consistent with Akt promoting cell cycle entry, G1 progression and/or the G1/S transition.

ISC/p cell overproduction and intestinal polyposis initiation

PTEN loss results in a higher number and altered distribution of the M^+ISC/p cell population. This increase could simply be due to their increased proliferation but might also involve more frequent symmetric division. Changes in the M^+ISC/p distribution may be due to the mutant stem cells being more mobile, consistent with the known role of Akt in governing cell migration[16]. Alternatively, descendents of PTEN-deficient ISCs may retain or reacquire ISC properties, yielding aberrantly localized M^+ISC/p cells, a process possibly involving secondary mutation. The behavior of PTEN-deficient ISCs resembles that of PTEN-deficient hematopoietic stem cells, which cycle more actively than normal and are impaired in their ability to lodge in bone marrow niches[29]. We conclude that in stem cell populations, PTEN functions to negatively regulate the cell cycle[29,40,41] and that sometimes this is coupled with control of stem cell location[29].

Both crypt fission and crypt budding feature M^+ISC/p cells at the initiation site, indicating a central role for these stem cells in the initiation of polyposis. Crypt fission, a component of normal intestinal growth and repair as well as a feature of polyposis, has been suggested to occur when the number of ISCs in a crypt exceeds some threshold capacity[7], and our data validate this concept. Similarly, we propose that aberrantly located $Musashi^+$ cells direct the *de novo* budding morphogenesis of crypt-like structures from existing villi or crypts. This budding process will probably share some of the molecular and cellular characteristics of the initial formation of crypts during intestinal development, in which $Musashi^+$ cells demonstrate a similar distribution[24,42].

Wnt and PTEN-Akt pathways cooperate in ISC activation

The nuclear localization of β-catenin is considered a critical event in stem cell activation and, therefore, for homeostasis of the intestine[9,36]. The highly restricted intestinal patterns of

nuclear β-catenin and its transcription activity (shown by Top-Gal) are puzzling, as many Wnt-pathway components are expressed rather broadly or in gradients[43], and the widespread distribution of the phosphorylated form of Wnt coreceptor Lrp6 suggests that all proliferating cells in crypts are exposed to Wnt signaling[9]. Akt, active in M^+ISC/p cells, assists the Wnt pathway in regulating nuclear localization of β-catenin[9] and may provide spatial specificity. We have now identified the molecular link between β-catenin nuclear localization and the activity of the PTEN-Akt pathway. Akt phosphorylates β-catenin at Ser552, and the resulting p-β-cat-Ser552 form has a nuclear distribution. We also find that PTEN loss results in an increase in the number of ISC/p cells with nuclear β-catenin as well as higher levels of nuclear p-β-cat-Ser552. Moreover, ISC/p cells participating in crypt fission and crypt budding have nuclear p-β-cat-Ser552.

Precisely how phosphorylation of Ser552 influences the nuclear localization of β-catenin remains to be determined. On balance, phosphorylation of this single site may not be the sole, or even primary, determinant of β-catenin localization. Instead, we expect that additional modifications, perhaps including Akt phosphorylation at Thr217, Thr332 or Ser675, are required. The position of Ser552 within a flexible insertion interrupting Armadillo repeat (R)10 (ref. 44) does, however, suggest mechanisms by which phosphorylation at the Akt target site might participate in localization. The C-terminal portion of the protein, including R10, is implicated in the nuclear import and export of β-catenin[45], and it is also suggested that conformational changes in this region help partition β-catenin between nuclear and membrane pools[46]. Phosphorylation of Ser552 may therefore modulate the translocation of β-catenin through nuclear pores or affect its conformation[47,48]. Another possibility to consider is that phosphorylation by Akt occurs within the nucleus[49] and affects function rather than localization. Indeed, Ser552 and Ser675 are also targets of PKA[50], and mutation of the codons encoding these sites influences transcriptional activity of β-catenin more than its localization[50]. Thus, further studies are required to clarify the functional role of Akt phosphorylation of β-catenin in M^+ISC/p cells.

PTEN loss removes a single negative regulator from the PI3K/Akt pathway, but the activity of this pathway is still restrained by controlling the input (signals stimulating PI3K) and by additional negative regulators. Coordination of Akt signaling with the Wnt/β-catenin pathway suggests that PTEN loss could have rather limited impact on M^+ISC/p cells unless the PI3K and Wnt pathways are both stimulated. The localized polyposis within PTEN mutant epithelium might thus reflect sites where further dysregulation of either PI3K or Wnt signaling has occurred.

Clinical implications of the stem cell origin of polyposis

An ideal cancer therapy would target cancer stem cells but not normal stem cells, but developing such a treatment requires better knowledge of the properties of both. The activity of the PTEN-Akt pathway is one distinction between these states. PTEN loss leads to an excess of overly proliferative ISC/p cells that seed the initiation of polyps, findings that bring us closer to understanding how stem cell behavior is controlled and how mutant stem cells contribute to neoplasia.

METHODS

Animal model

All animal work was performed in compliance with protocols approved by the Institutional Animal Care and Use Committee at Stowers Institute for Medical Research. We induced PTEN conditional inactivation by injecting polyinosinic-polycytidylic acid five to seven times following the procedure described previously[9] and verified targeting efficiency by PCR (**Supplementary Methods** online).

Tissue preparation, immunostaining and protein blot analyses

Minor modifications of the antibodies and procedures described in our previous report[9] were used here. Staining conditions for new antibodies and detailed procedures for immunohistochemical staining of nuclear β-catenin are described in **Supplementary Methods**. Details for protein blot analysis, Top-Gal staining and the generation and purification of the anti-p-β-catenin-Ser552 antibody are also described in **Supplementary Methods**.

Whole-mount immunofluorescent staining

Isolated intestinal crypts were fixed in 4% paraformaldehyde for 1 h at 4 °C and permeabilized using 0.5% Triton X-100 in PBS. Staining was performed as described in **Supplementary Methods**.

Bioinformatics and mass spectrometry

To identify potential Akt phosphorylation sites in β-catenin, we used Scansite 2.0 (**Supplementary Methods**) and performed a medium-stringency motif search of the human β-catenin protein sequence, which identified a single potential Akt (basophilic serinethreonine kinase) phosphorylation site at Ser552. The collision-induced dissociation spectrum for the peptide spanning Ser552 showed a major peak representing the loss of the 98-Da H_3PO_4 group from the parent ion, indicating that Ser552 is phosphorylated by Akt (see Results and **Supplementary Methods**).

Microarray and RT-PCR assays

The procedures for both microarray and RT-PCR assays have been previously described (**Supplementary Methods**). Microarray analysis compared the gene expression profiles of polyp regions from three PTEN-deficient animals with intestines from two controls. The programs used for gene expression analyses and gene ontology analysis are described in **Supplementary Methods**.

Supplementary Material

Refer to Web version on PubMed Central for supplementary material.

ACKNOWLEDGMENTS

We are grateful to B. Neaves and R. Krumlauf for scientific support. We thank H. Okano for providing anti-Musashi1 (14-H1) and A. Ouellette for anti-cryptdin; S. Peck and G. Yang for comments on the manuscript; D. di

Natale for assistance on manuscript editing; P. Kulesa and D. Stark for imaging assistance; C. Seidel, K. Zueckert-Gaudenz and M. Coleman for assistance in microarray analysis; H. Marshall for technology support and J. Chen for assistance in statistical analysis. L. Li is supported in part by research grant 5-FY05-31 from the March of Dimes Birth Defects Foundation, by grant R01 DK070001 from the National Institute of Diabetes and Digestive and Kidney Diseases and by the Stowers Institute for Medical Research.

References

1. Reya T, Morrison SJ, Clarke MF, Weissman IL. Stem cells, cancer, and cancer stem cells. Nature. 2001; 414:105–111. [PubMed: 11689955]
2. Lapidot T, et al. A cell initiating human acute myeloid leukaemia after transplantation into SCID mice. Nature. 1994; 367:645–648. [PubMed: 7509044]
3. Al-Hajj M, Wicha MS, Benito-Hernandez A, Morrison SJ, Clarke MF. Prospective identification of tumorigenic breast cancer cells. Proc. Natl. Acad. Sci. USA. 2003; 100:3983–3988. [PubMed: 12629218]
4. Singh SK, et al. Identification of human brain tumour initiating cells. Nature. 2004; 432:396–401. [PubMed: 15549107]
5. Potten CS, Owen G, Booth D. Intestinal stem cells protect their genome by selective segregation of template DNA strands. J. Cell Sci. 2002; 115:2381–2388. [PubMed: 12006622]
6. Radtke F, Clevers H. Self-renewal and cancer of the gut: two sides of a coin. Science. 2005; 307:1904–1909. [PubMed: 15790842]
7. Brittan M, Wright NA. Gastrointestinal stem cells. J. Pathol. 2002; 197:492–509. [PubMed: 12115865]
8. Bjerknes M, Cheng H. Clonal analysis of mouse intestinal epithelial progenitors. Gastroenterology. 1999; 116:7–14. [PubMed: 9869596]
9. He XC, et al. BMP signaling inhibits intestinal stem cell self-renewal through suppression of Wnt-beta-catenin signaling. Nat. Genet. 2004; 36:1117–1121. [PubMed: 15378062]
10. Haramis AP, et al. *De novo* crypt formation and juvenile polyposis on BMP inhibition in mouse intestine. Science. 2004; 303:1684–1686. [PubMed: 15017003]
11. Greaves LC, et al. Mitochondrial DNA mutations are established in human colonic stem cells, and mutated clones expand by crypt fission. Proc. Natl. Acad. Sci. USA. 2006; 103:714–719. [PubMed: 16407113]
12. Howe JR, et al. Germline mutations of the gene encoding bone morphogenetic protein receptor 1A in juvenile polyposis. Nat. Genet. 2001; 28:184–187. [PubMed: 11381269]
13. Sancho E, Batlle E, Clevers H. Signaling pathways in intestinal development and cancer. Annu. Rev. Cell Dev. Biol. 2004; 20:695–723. [PubMed: 15473857]
14. van de Wetering M, et al. The beta-catenin/TCF-4 complex imposes a crypt progenitor phenotype on colorectal cancer cells. Cell. 2002; 111:241–250. [PubMed: 12408868]
15. Liaw D, et al. Germline mutations of the *PTEN* gene in Cowden disease, an inherited breast and thyroid cancer syndrome. Nat. Genet. 1997; 16:64–67. [PubMed: 9140396]
16. Stiles B, Groszer M, Wang S, Jiao J, Wu H. PTENless means more. Dev. Biol. 2004; 273:175–184. [PubMed: 15328005]
17. Zhou XP, et al. Germline mutations in *BMPR1A/ALK3* cause a subset of cases of juvenile polyposis syndrome and of Cowden and Bannayan-Riley-Ruvalcaba syndromes. Am. J. Hum. Genet. 2001; 69:704–711. [PubMed: 11536076]
18. Waite KA, Eng C. BMP2 exposure results in decreased PTEN protein degradation and increased PTEN levels. Hum. Mol. Genet. 2003; 12:679–684. [PubMed: 12620973]
19. Tian Q, et al. Proteomic analysis identifies that 14–3-3ζ interacts with β-catenin and facilitates its activation by Akt. Proc. Natl. Acad. Sci. USA. 2004; 101:15370–15375. [PubMed: 15492215]
20. Persad S, Troussard AA, McPhee TR, Mulholland DJ, Dedhar S. Tumor suppressor PTEN inhibits nuclear accumulation of beta-catenin and T cell/lymphoid enhancer factor 1-mediated transcriptional activation. J. Cell Biol. 2001; 153:1161–1174. [PubMed: 11402061]

21. Sharma M, Chuang WW, Sun Z. Phosphatidylinositol 3-kinase/Akt stimulates androgen pathway through GSK3beta inhibition and nuclear beta-catenin accumulation. J. Biol. Chem. 2002; 277:30935–30941. [PubMed: 12063252]
22. Groszer M, et al. Negative regulation of neural stem/progenitor cell proliferation by the Pten tumor suppressor gene *in vivo*. Science. 2001; 294:2186–2189. [PubMed: 11691952]
23. Kühn R, Schwenk F, Aguet M, Rajewsky K. Inducible gene targeting in mice. Science. 1995; 269:1427–1429. [PubMed: 7660125]
24. Potten CS, et al. Identification of a putative intestinal stem cell and early lineage marker; musashi-1. Differentiation. 2003; 71:28–41. [PubMed: 12558601]
25. Wirtzfeld DA, Petrelli NJ, Rodriguez-Bigas MA. Hamartomatous polyposis syndromes: molecular genetics, neoplastic risk, and surveillance recommendations. Ann. Surg. Oncol. 2001; 8:319–327. [PubMed: 11352305]
26. Vazquez F, et al. Phosphorylation of the PTEN tail acts as an inhibitory switch by preventing its recruitment into a protein complex. J. Biol. Chem. 2001; 276:48627–48630. [PubMed: 11707428]
27. Gera JF, et al. AKT activity determines sensitivity to mammalian target of rapamycin (mTOR) inhibitors by regulating cyclin D1 and c-myc expression. J. Biol. Chem. 2004; 279:2737–2746. [PubMed: 14576155]
28. Passegue E, Wagner EF, Weissman IL. JunB deficiency leads to a myeloproliferative disorder arising from hematopoietic stem cells. Cell. 2004; 119:431–443. [PubMed: 15507213]
29. Zhang J, et al. PTEN maintains hematopoietic stem cells and acts in lineage choice and leukaemia prevention. Nature. 2006; 441:518–522. [PubMed: 16633340]
30. Wasan HS, et al. APC in the regulation of intestinal crypt fission. J. Pathol. 1998; 185:246–255. [PubMed: 9771477]
31. Wong WM, et al. Histogenesis of human colorectal adenomas and hyperplastic polyps: the role of cell proliferation and crypt fission. Gut. 2002; 50:212–217. [PubMed: 11788562]
32. Preston SL, et al. Bottom-up histogenesis of colorectal adenomas: origin in the monocryptal adenoma and initial expansion by crypt fission. Cancer Res. 2003; 63:3819–3825. [PubMed: 12839979]
33. Shih IM, et al. Top-down morphogenesis of colorectal tumors. Proc. Natl. Acad. Sci. USA. 2001; 98:2640–2645. [PubMed: 11226292]
34. Tetsu O, McCormick F. Beta-catenin regulates expression of cyclin D1 in colon carcinoma cells. Nature. 1999; 398:422–426. [PubMed: 10201372]
35. Liang J, et al. PKB/Akt phosphorylates p27, impairs nuclear import of p27 and opposes p27-mediated G1 arrest. Nat. Med. 2002; 8:1153–1160. [PubMed: 12244302]
36. Lowry WE, et al. Defining the impact of β-catenin/Tcf transactivation on epithelial stem cells. Genes Dev. 2005; 19:1596–1611. [PubMed: 15961525]
37. Cross DA, Alessi DR, Cohen P, Andjelkovich M, Hemmings BA. Inhibition of glycogen synthase kinase-3 by insulin mediated by protein kinase B. Nature. 1995; 378:785–789. [PubMed: 8524413]
38. Datta SR, et al. 14–3-3 proteins and survival kinases cooperate to inactivate BAD by BH3 domain phosphorylation. Mol. Cell. 2000; 6:41–51. [PubMed: 10949026]
39. van Noort M, Meeldijk J, van der Zee R, Destree O, Clevers H. Wnt signaling controls the phosphorylation status of beta-catenin. J. Biol. Chem. 2002; 277:17901–17905. [PubMed: 11834740]
40. Groszer M, et al. PTEN negatively regulates neural stem cell self-renewal by modulating G0–G1 cell cycle entry. Proc. Natl. Acad. Sci. USA. 2006; 103:111–116. [PubMed: 16373498]
41. Yilmaz OH, et al. Pten dependence distinguishes haematopoietic stem cells from leukaemia-initiating cells. Nature. 2006; 441:475–482. [PubMed: 16598206]
42. Asai R, Okano H, Yasugi S. Correlation between Musashi-1 and c-hairy-1 expression and cell proliferation activity in the developing intestine and stomach of both chicken and mouse. Dev. Growth Differ. 2005; 47:501–510. [PubMed: 16287482]
43. Gregorieff A, et al. Expression pattern of Wnt signaling components in the adult intestine. Gastroenterology. 2005; 129:626–638. [PubMed: 16083717]

44. Huber AH, Nelson WJ, Weis WI. Three-dimensional structure of the Armadillo repeat region of β-catenin. Cell. 1997; 90:871–882. [PubMed: 9298899]

45. Koike M. β-catenin shows an overlapping sequence requirement but distinct molecular interactions for its bidirectional passage through nuclear pores. J. Biol. Chem. 2004; 279:34038–34047. [PubMed: 15173161]

46. Gottardi CJ, Gumbiner BM. Distinct molecular forms of beta-catenin are targeted to adhesive or transcriptional complexes. J. Cell Biol. 2004; 167:339–349. [PubMed: 15492040]

47. Piedra J, et al. Regulation of beta-catenin structure and activity by tyrosine phosphorylation. J. Biol. Chem. 2001; 276:20436–20443. [PubMed: 11279024]

48. Megy S, et al. Solution structure of a peptide derived from the oncogenic protein β-catenin in its phosphorylated and nonphosphorylated states. Peptides. 2005; 26:227–241. [PubMed: 15629534]

49. Trotman LC, et al. Identification of a tumour suppressor network opposing nuclear Akt function. Nature. 2006; 441:523–527. [PubMed: 16680151]

50. Taurin S, Sandbo N, Qin Y, Browning D, Dulin NO. Phosphorylation of beta-catenin by cyclic AMP-dependent protein kinase. J. Biol. Chem. 2006; 281:9971–9976. [PubMed: 16476742]

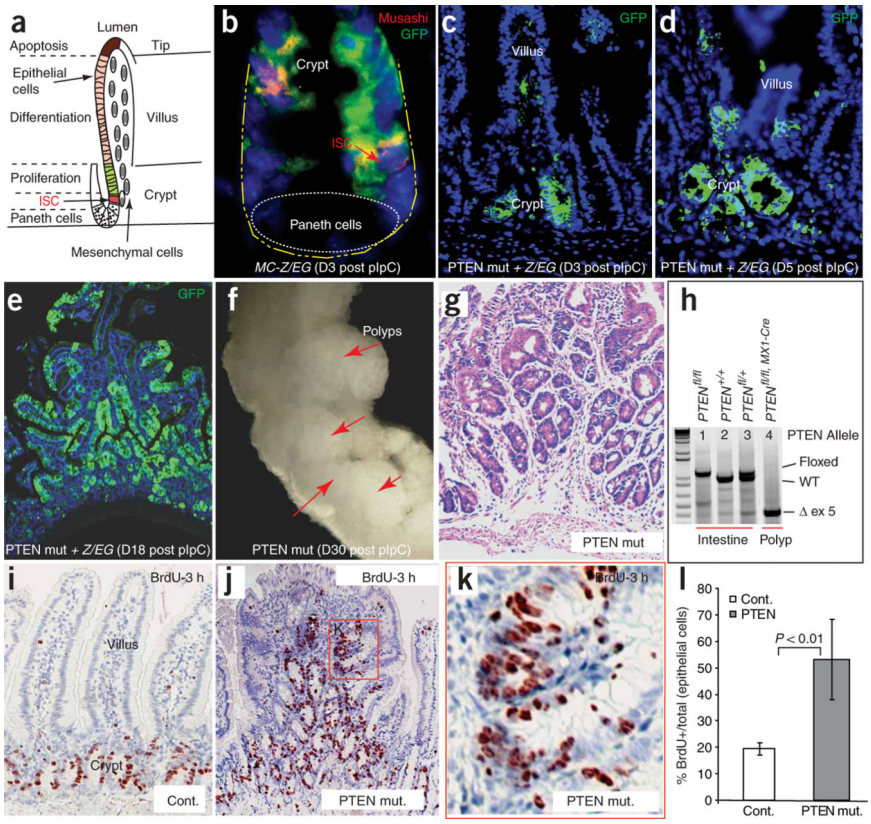

Figure 1.

Inactivation of PTEN leads to intestinal polyposis. (**a**) Illustration of crypt and villus regions of intestines in which intestinal stem cells (ISCs), proliferating progenitor cells and differentiated cells are located in spatially defined compartments. (**b–e**) Histology slides showing Cre expression and targeting efficiency in crypt cells, including ISC (red arrow in **b** represents Musashi^{+} cells) using the compound genetic mouse model *Mx1-Cre*$^{+}$*;Pten*$^{fl/fl}$*;Z/EG*. Green staining is present where Cre activity has deleted the PTEN gene and activated GFP in the reporter. The number of days after pIpC induction is shown in parentheses. (**f**) PCR confirmation of successful targeting of the PTEN gene. Lane 1, homozygote with both *Pten* alleles flanked by *LoxP* sites; Lane 2, wild-type (Wt) line; Lane 3, heterozygote; Lane 4, efficient deletion of exon5 (ex5) in the *Pten* locus. (**g**) Photograph of multiple intestinal polyps formed in the PTEN mutant animals. (**h**) Stained histology slide of a polyp from a *Pten*-deficient mouse one month after pIpC injection. (**i–k**) Comparison of the proliferation zones, as measured by 3-h BrdU-pulse labeling, in the intestines of control and *Pten*-deficient mice. **k** shows the boxed region in **j** at higher magnification. (**l**) Comparison of the proliferation index of control and *Pten*-deficient mice. Error bars represent s.d.

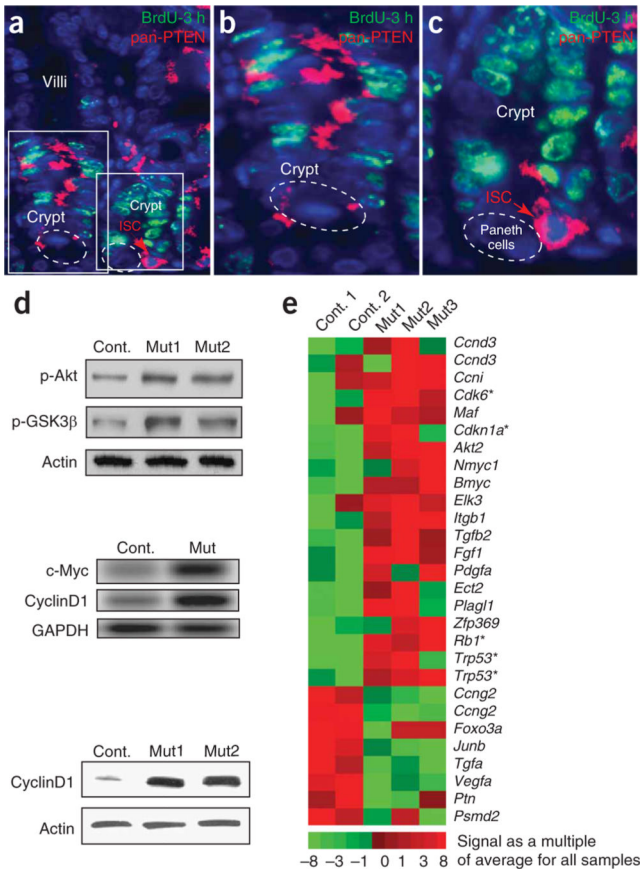

Figure 2.

PTEN expression in the intestine and the impact of PTEN inactivation on the activity of the PI3K-Akt pathway and on the expression of cell cycle regulators. (**a–c**) Dual immunofluorescence using a pan-PTEN antibody to detect both p-PTEN and non-p-PTEN and an antibody to BrdU to detect pulse-labeled cells. PTEN protein is detected in portions of the transit amplification compartment that are not actively cycling (**b**). PTEN is also highly expressed in the ISC position (**c**). The left and right boxes in **a** are shown at higher magnification in **b** and **c**, respectively. (**d**) Protein blot and RT-PCR analysis of PTEN-deficient intestine. Top and bottom panels (protein blots) demonstrate increased levels of p-Akt and p-GSK3β (top) and cyclinD1 (bottom). An RT-PCR assay also showed increased levels of Myc and cyclinD1 (center panel). (**e**) Microarray assay analysis showing changes in cell cycle-related genes in the PTEN-deficient mouse. Heat map represents signal of an individual sample relative to the average of all five samples. Asterisk indicates genes identified with the BioCarta term ‘cell cycle: G1/S checkpoint’.

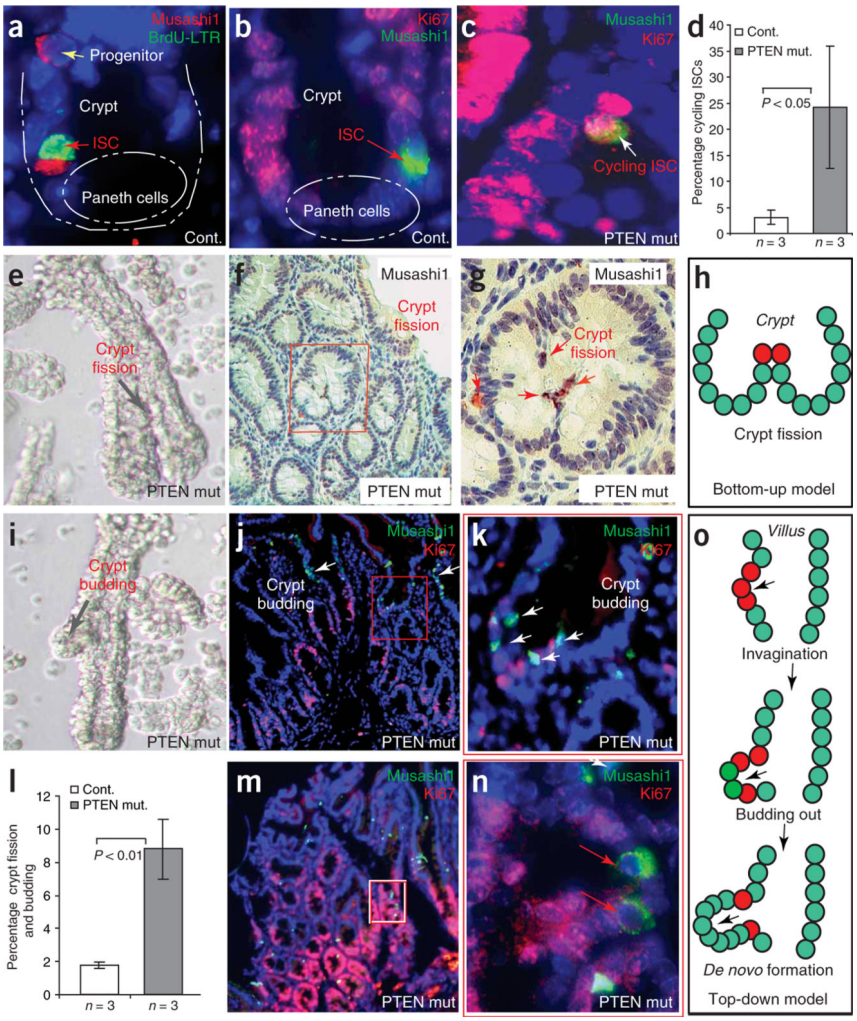

Figure 3.

PTEN-deficient intestinal stem cells were found at the initiation of crypt budding and fission. (**a**) Association of Musashi1 (red), with BrdU (BrdU-LTR; green) cells in control mice. (**b**) In control mice, ISCs, identified as Musashi1^{+} (green) are in most cases Ki67^{-} and therefore slow cycling. (**c,d**) The percentage of double-positive (Musashi1^{+} Ki67^{+}) cells was higher in PTEN-deficient intestine. (**e**) Microdissected crypt showing crypt fission in the PTEN-deficient intestine. (**f,g**) M^{+}ISC/p cells are detected in the apex of bifurcated fission crypts. Boxed area in **f** is shown at higher magnification in **g**. (**h**) A schematic showing the relationship between M^{+}ISC/p cells (red) and crypt fission. (**i**) Microdissected crypt showing crypt budding in the PTEN-deficient intestine. (**j,k**) M^{+}ISC/p cells found at the initiation point of crypt budding or *de novo* crypt formation. White arrows indicate clusters of M^{+}ISC/p cells detected in a region undergoing invagination (**j**) and budding (**k**). The boxed area in **j** shows a newly formed crypt (shown at higher magnification in **k**). (**l**) Graph showing increased percentage of crypt fission and budding in the PTEN mutants. (**m,n**) Increase in M^{+}ISC/p cells in the polyp region (M) and duplicate M^{+}ISC/p cells in the newly formed crypt (**n**). The majority of M^{+}ISC/p cells in the polyp region are Ki67^{-} (**n**). Boxed

area in **m** is shown at higher magnification in **n**. (**o**) Model of involvement of M^+ISC/p cells (red) in *de novo* crypt formation in the PTEN-deficient polyp region.

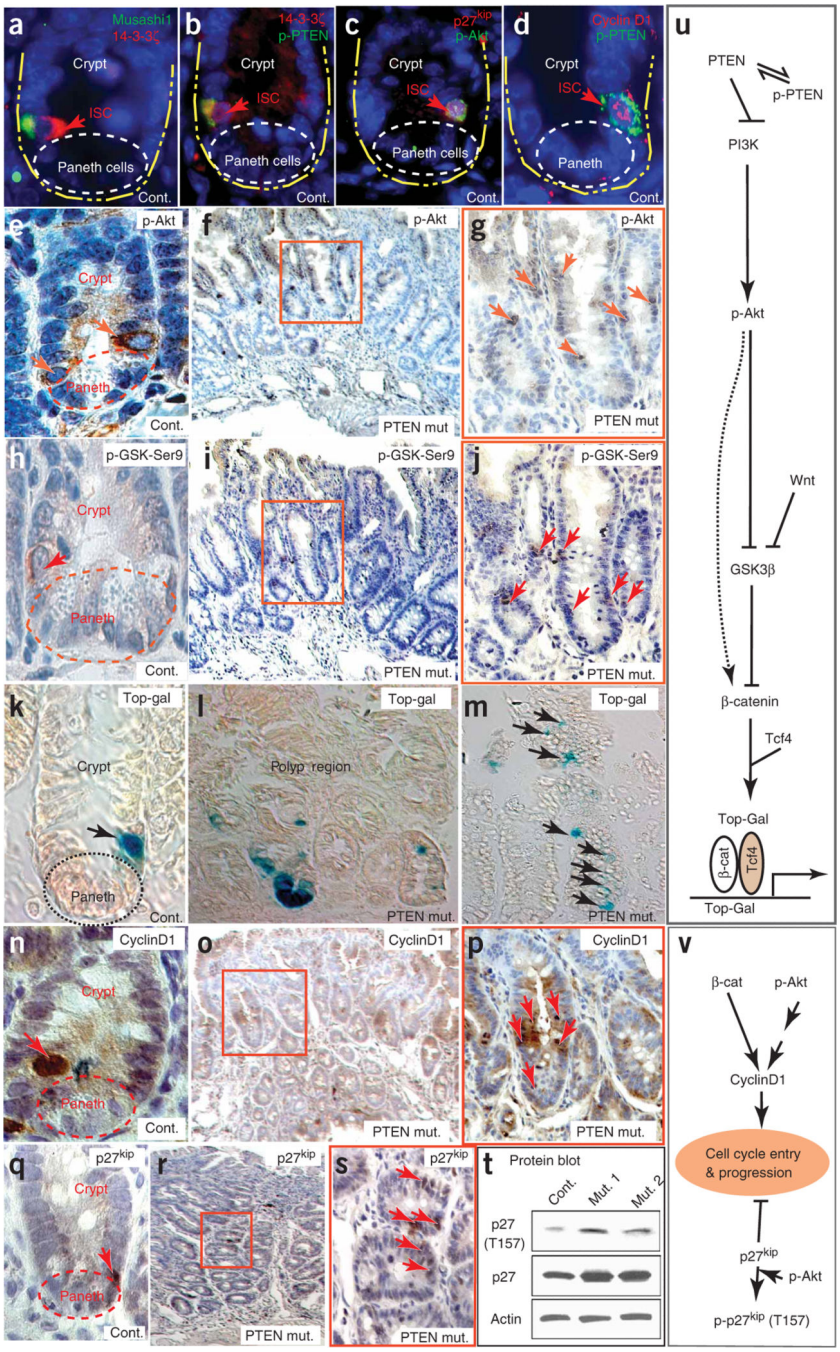

Figure 4.

PI3K-Akt pathway and its downstream targets operate in ISCs when PTEN is inactivated. (**a–d**) Expression of Musashi1, components of the PTEN-Akt pathway and nuclear cyclinD1 in ISCs. Musashi1 colocalizes with 14-3-3ζ (**a**) and p-PTEN (**b**). PTEN-Akt signaling in ISCs is associated with nuclear $p27^{kip1}$ or nuclear plus cytoplasmic $p27^{kip1}$ (**c**) and nuclear cyclinD1 (**d**). (**e–j**) The number of p-Akt^{+} (**e–g**) and p-GSK3β-$Ser9^{+}$ (**h–j**) cells is higher in the polyp regions of the PTEN-deficient mice (**f,g,i–j**) than in intestine from control mice (**e,h**). Red arrows indicate strongly positive cells. **f,g** and **i–j** are adjacent sections from the

same polyp. Control sections show that cells at the ISC position are strongly positive for p-Akt (**e**) and p-GSK3β-Ser9 (**h**). Boxed areas in **f** and **i** are shown at higher magnification in **g** and **j**, respectively. (**k–m**) Top-Gal detects cells with β-catenin transcriptional activity, found mainly in cells at the stem and Paneth cell positions in control mice but in multiple places in PTEN-deficient mice (**Supplementary Fig. 4**). (**n–p**) The number of cells with a high level of nuclear cyclinD1 was higher in the polyp region of PTEN-deficient mice (**o–p**) than in the control (**n**). Boxed area in **o** is shown at higher magnification in **p**. (**q–s**) The number of cells with nuclear $p27^{kip1}$ (red arrows) was higher in the polyp region of PTEN mutants (**r,s**) than in control intestine (**q**). Boxed area in **r** is shown at higher magnification in **s**. (**t**) Protein blot comparison of the amount and phosphorylation state of $p27^{kip1}$ in control intestines and PTEN-deficient polyps. (**u**) Illustration of the PTEN-Akt signaling pathway that assists Wnt in controlling β-catenin activity. (**v**) Illustration of the PTEN-Akt signaling pathway that controls cell cycle entry and progression.

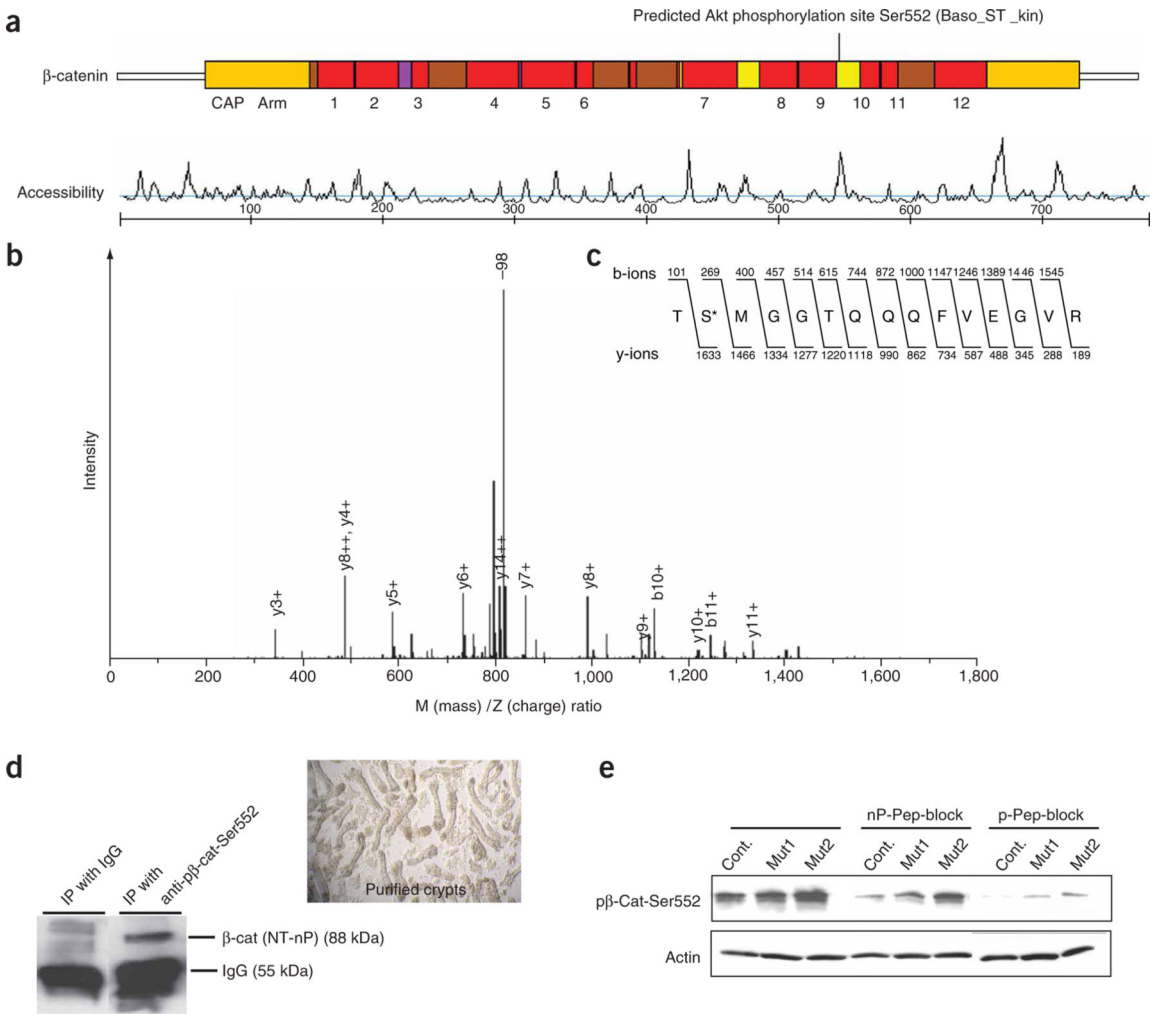

Figure 5.

Identification of the Akt phosphorylation site at the C terminus of β-catenin. (**a**) Scansite 2.0 output identifying Ser552 as a putative Akt phosphorylation site (basophilic serine-threonine kinase site) at the C terminus of β-catenin. The site is located in the 10th of the 12 armadillo (Arm) repeats and has high accessibility. (**b**) Mass spectrometry analysis identified a phosphorylated peptide generated by incubation of β-catenin protein with activated Akt. A high-intensity peak corresponding to loss of 98 Da (–98) is indicative of phosphorylation. Additional peaks correspond to the b- and y-ions expected for the peptide shown in **c**. (**c**) Amino acid sequence of the β-catenin peptide identified as containing an Akt phosphorylation site, showing the masses of the expected b- and y-ions. The asterisk marks the phosphorylated Ser552. (**d**) Confirmation that anti-p-β-cat-Ser552, recognizes the active form of β-catenin. Immunoprecipitation (IP) was performed using anti-p-β-cat-Ser552 or IgG as a control and subsequently blotted using an antibody to N-terminally nonphosphorylated β-catenin (NT-nP) from purified crypts. Image at right shows purified crypts used for the IP assay. (**e**) Protein blot determination of the specificity of anti-p-β-cat-Ser552 using nonphosphorylated (nP) and phosphorylated (p) peptide block.

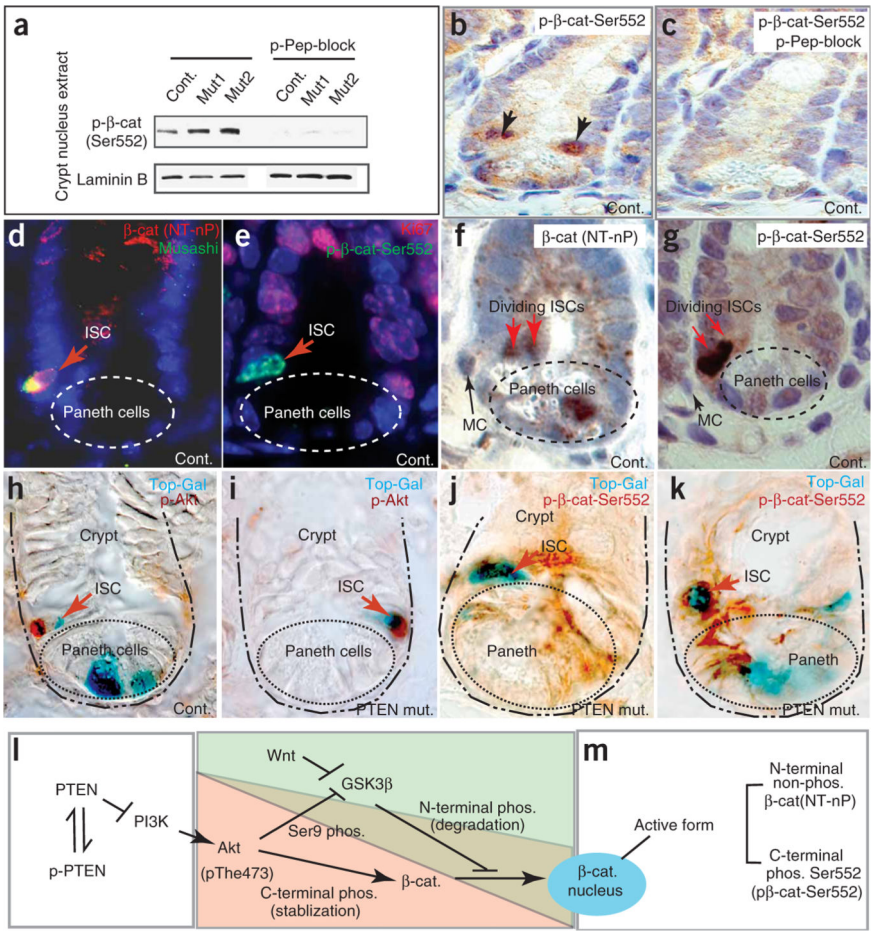

Figure 6.

Akt activity coincides with nuclear p-β-cat-Ser552 and β-catenin–dependent transcriptional activity in ISCs. (**a**) Protein blot analyses comparing the protein levels of nuclear β-catenin in crypt nuclear extract in control and PTEN-deficient intestines. A phosphorylated peptide (p-Pep) blocker was able to specifically inhibit binding of β-catenin by anti-p-β-cat-Ser552. (**b,c**) Cells at the stem cell position have nuclear p-β-cat-Ser552 (**b**). Signal detected by anti-p-β-cat-Ser552 can be blocked by a phosphorylated peptide blocker (**c**). (**d–g**) Distribution pattern of β-catenin in crypts as detected by an antibody to the N-terminally nonphosphorylated form (NT-nP) (**d,f**) and anti-p-β-cat-Ser552 (**e,g**). Red arrows indicate ISC position (**d,e**) and dividing ISCs (**f,g**). MC: mesenchymal cell. (**h–k**) Active Akt and nuclear p-β-cat-Ser552 correlated with Top-Gal activity in some crypt cells, including ISCs. Control: *Mx1-Cre*$^{+}$*:Pten*$^{fl/+}$. 'PTEN mut': **Mx1-Cre**$^{+}$**: Pten**$^{fl/fl}$. (**l,m**) Illustration of the regulation of nuclear β-catenin by Wnt and Akt pathways, suggesting a relationship between phosphorylation and nuclear activity of β-catenin. Nuclear-localized forms of β-catenin are identified by nonphosphorylation at the N terminus, by C-terminal phosphorylation at Ser552, or both.

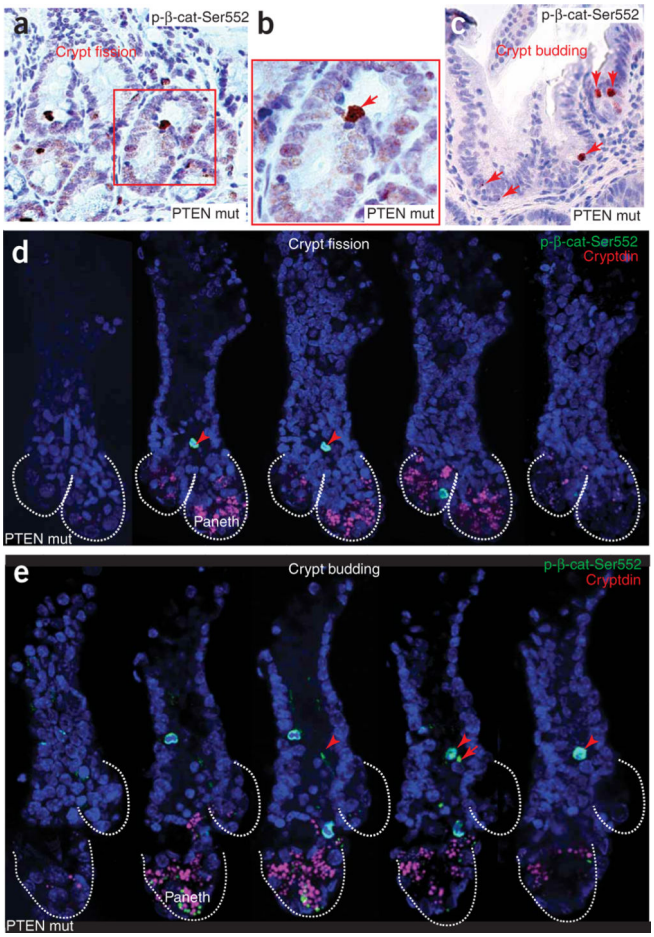

Figure 7.

Cells with nuclear p-β-cat-Ser552 initiate crypt fission and budding. (**a–c**) In PTEN-deficient polyps, a cluster of cells with nuclear p-β-cat-Ser552 was found at the apex of the ridge of dividing crypts in crypt fission (**a,b**) and at the point of initiation of a budding crypt (**c**). (**d,e**) Serial view of a dividing crypt (fission) (**d**) and a budding crypt (**e**) in the PTEN mutants, detected using a confocal *Z*-stack in which cells with nuclear p-β-cat-Ser552 were found at the point of initiation of fission or budding. Cryptdin was used to detect Paneth cells (see **Supplementary Videos 1** and **2**).